Supplementary Material for

Endovascular administration of magnetized nanocarriers targeting brain delivery after stroke.

Alba Grayston[1] et al.

[1]Neurovascular Research Laboratory, Vall d'Hebron Institut de Recerca, Universitat Autònoma de Barcelona (VHIR-UAB), 08035 Barcelona, Catalonia, Spain; [2]Institut de Ciència de Materials de Barcelona (ICMAB-CSIC), Campus UAB, 08193 Bellaterra, Catalonia, Spain; [3]Achucarro Basque Center for Neuroscience, Laboratory of Neuroimaging and biomarkers of inflammation, E-48940 Leioa, Spain; [4]Ikerbasque Basque Foundation for Science, 48013 Bilbao, Spain; [5]Institute of Experimental physics, SAS, 040 01 Kosice, Slovakia; [6]Biomedical Center Martin, Jessenius Faculty of Medicine in Martin, Comenius University in Bratislava, 036 01 Martin, Slovakia; [7]Department of Clinical Biochemistry, Clinical Laboratories, Vall d'Hebron University Hospital, 08035 Barcelona, Catalonia, Spain; [8]Nuclear Medicine Department, IRCCS San Raffaele Scientific Institute, 20132 Milan, Italy; [9]Institute of Molecular Bioimaging and Physiology (IBFM) of CNR, 20090 Segrate, Italy; [10]Department of Medicine and Surgery, University of Milano – Bicocca, 20126 Milan, Italy; [11]Vita-Salute San Raffaele University, 20132 Milan, Italy.

[*]**Corresponding Authors:** Anna Rosell: anna.rosell@vhir.org; Anna Roig: roig@icmab.es

Supplementary Methods

Validation for magnetic tracking

To test the efficacy of magnetic targeting of the magnet devices, a dust magnetic targeting test was performed as seen in Figure 5(c) of the main text. Ferrimagnetic magnetite microparticles (10 μm average diameter) were dispersed in mineral oil and each magnet device was placed at the center to test the covered distance of magnetic attraction of the magnetic microparticles.

The magnetic targeting efficacy was then validated for the focused magnet (M2) with a simple chicken egg model and MRI by tracking the position of an injected magnetic fluid. The magnetic fluid was prepared with magnetite particles (10 nm average diameter) covered by polyethylene glycol (PEG), a biocompatible polymer, dissolved in a physiological salt-based solution at a concentration of 0.305

mg/mL. The MRI measurements were performed by using a 7 T BioSpec Bruker system. T2*-weighted images (T2*WI) were acquired by Multi Gradient Echo (MGE) pulse sequence by using the following parameters: repetition time (TR) = 881 ms, starting echo time (TE) = 3 ms, echo-spacing = 3.41 ms (for 10 different TE), flip angle (FA) = 50°, 23 coronal slices of 1 mm slice thickness (ST) and 0.5 mm gap, field of view (FOV) = 70 x 58 mm, matrix size (MTX) = 256 x 256. The illustration of the experimental procedure for the effectivity of targeting can be seen in Figure S5 together with the magnetic fluid tracking and targeting towards the M2 position 45 min after injection.

FMI analysis

Background control animals who did not receive fluorescent NC were also imaged in each *in vivo* and *ex vivo* FMI acquisition for background measures. For quantification, circular regions of interest (ROIs) were manually drawn surrounding the fluorescence signal and total radiant efficiency (TRE; [photons/s]/[μW/cm²]) was measured using the Living Image software (Perkin Elmer, Waltham, MA) and corrected by the TRE from the corresponding ROI in the background control animal. More specifically, for the *in vivo* analysis, brain and abdominal ROIs were drawn on the dorsal and ventral images, respectively, and for the *ex vivo* analysis, ROIs of each dissected organ were drawn in both dorsal and ventral positions. All images were analyzed by a researcher blinded to the treatment group and mean values of both views were used for the analysis.

MRI acquisition protocols and analysis

Mice were anesthetized with isoflurane via facemask (5% for induction, 0.5-1.5% for maintenance in 1L/min O_2) with respiratory frequency monitoring and a recirculation water heating system integrated into the scanner bed was used to control the body temperature. T2-weighted fast spin-echo images were initially obtained in axial, sagittal and coronal planes to be used as reference images using the following parameters: effective echo time (TEeff) = 36 ms, TR = 2s, echo train length (ETL) = 8, FOV = 1.92×1.92 cm2, MTX = 128x128, and ST = 1 mm. Then, coronal high-resolution MRI sections were determined over a 9.3 mm block starting at the olfactory bulb and towards the cerebellum. High-resolution T2WI (HR-T2WI) were acquired using a fast spin-echo sequence with ETL = 8, TEeff / TR = 60 ms / 4.2 s, FOV=1.6x1.6 cm2, MTX = 256x256, 17 contiguous slices with ST = 0.5 mm and 0.05 mm gap between them. High-resolution T2*WI (HR-T2*WI) were acquired using a spoiled gradient-echo sequence with TEeff / TR = 10.5 ms / 350 ms, FA = 40°, FOV = 1.6x1.6 cm2, MTX = 320x320,

17 slices covering the same brain region as in HR-T2WI with ST = 0.5 mm and 0.05 mm gap between them.

The superparamagnetic properties of the SPION embedded in the surface of the NC show good performance as transverse relaxation (T2) contrast agents, thus facilitating NC tissue tracking as hypointense signal spots. To quantify the amount of NC present in the brain after endovascular-ICA administration, ROIs were drawn dividing the cortical and subcortical areas of the ipsilateral and contralateral brain hemispheres on the T2*WI. After a standardized preprocessing of the images, the number, area, and average size of the NC hypointense signals within each ROI were analyzed using the particle analysis tool from the ImageJ software. All images were analyzed by a researcher blinded to the treatment group.

Functional tests

Neurological score ranges from 0 (healthy) to 39 and represents the sum of the general deficits (0-13): hair [0-2], ears [0-2], eyes [0-3], posture [0-3] spontaneous activity [0-3]; and focal deficits (0-26): body symmetry [0-2], gait [0-4], climbing on a surface held at 45º [0-3], circling behavior [0-3], front limb symmetry [0-4], compulsory circling [0-3], whiskers response to a light touch [0-4] and gripping of the forepaws [0-3]. The forelimb force was assessed as follows: habituation to the test was performed one day prior to the surgery to avoid neophobic behaviors and the grip strength was measured before the surgery and at 24 h and 48 h after MCAo. The grip strength score was recorded as the mean of 6 repeated measures.

Biochemical analysis

Liver/pancreas/renal toxicity was assessed by the plasmatic levels of ALT, AST, CK, α-amylase, lipase, creatinine, urea, and sodium using an Olympus AU5800 clinical chemistry analyzer. Hemolyzed, icteric and lipemic plasma samples were rejected from the analysis of the biochemical parameters described above.

Table S1. Summary of the PLGA-based NC. Size and dispersion characteristics of each batch of NC were measured by DLS.

Batch ID	Z-Average (nm)	PdI
PLGA_SPION_Cy7.5		
NC1	267.0	0.267
NC2	372.7	0.332
NC3	283.7	0.226
NC4	270.5	0.144
NC5	260.1	0.109
NC6	252.6	0.157
NC7	255.4	0.205
NC8	256.5	0.055
NC9	261.1	0.044
NC10	266.5	0.210
Mean	**277.0**	**0.175**
SD	**36.9**	**0.091**
PLGA_SPION		
NC11	248.2	0.145
NC12	267.9	0.166
NC13	268.4	0.137
NC14	282.5	0.129
Mean	**266.2**	**0.144**
SD	**17.2**	**0.016**

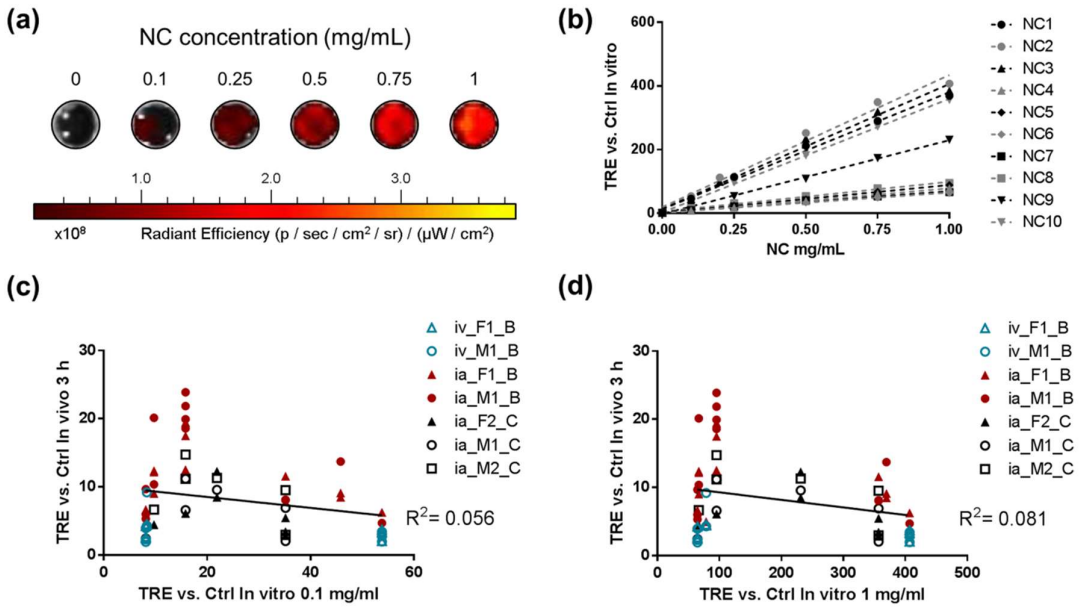

Figure S1. Cy7.5_NC batches fluorescence *in vitro*. (a) Representative FMI images of increasing concentrations of Cy7.5_NC dispersed in saline. (b) Quantification of TRE on ROIs drawn for each plate well at increasing NC concentrations, corrected by TRE from the corresponding control well containing saline. (c) Correlation between TRE on brain ROIs quantified by FMI *in vivo* at 3 h after Cy7.5_NC injection and the TRE quantified by FMI *in vitro* of the corresponding Cy7.5_NC batch at 0.1 mg/mL. (d) Correlation between TRE on brain ROIs quantified by FMI *in vivo* at 3 h after Cy7.5_NC injection and the TRE quantified by FMI *in vitro* of the corresponding Cy7.5_NC batch at 1 mg/mL.

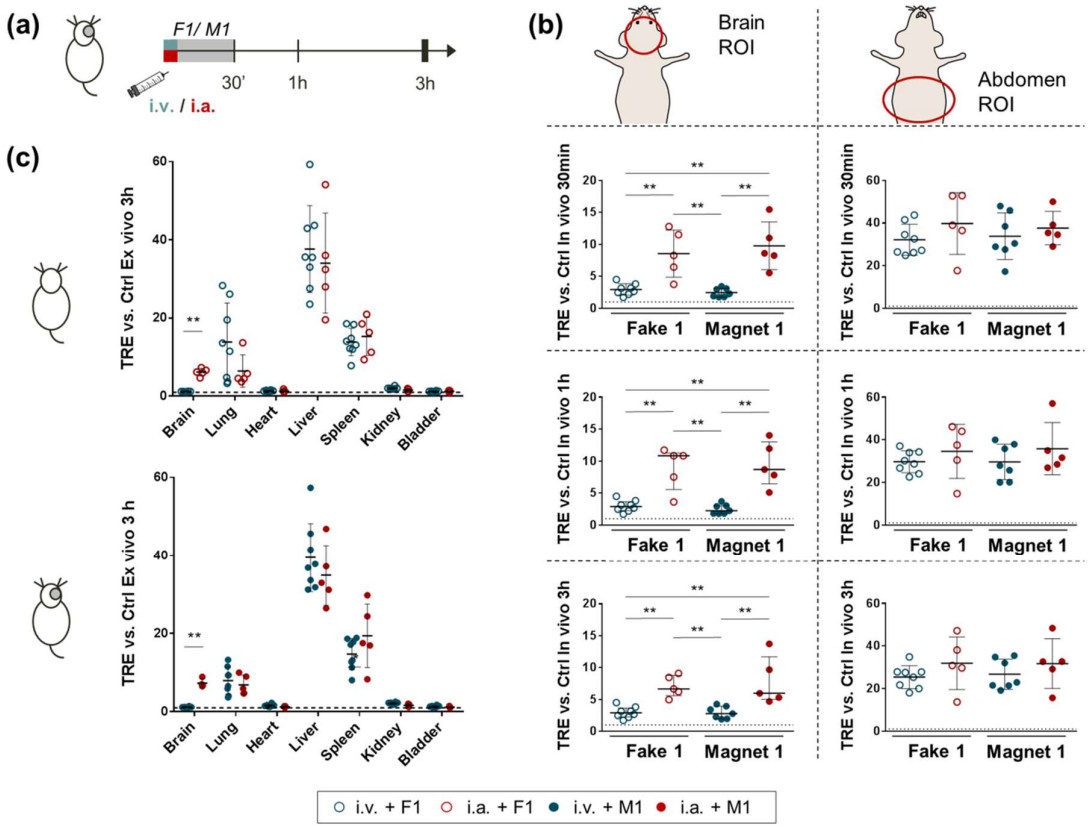

Figure S2. Complementary *Biodistribution study 1* data. (a) Scheme of the experimental design. (b) Graphs showing the TRE quantification on brain (left panel) and abdominal (right panel) ROIs from *in vivo* FMI acquisitions at 30 min, 1 h and 3 h after NC administration. (c) Graphs showing the TRE quantification on brain, lungs, heart, liver, spleen, kidneys, and bladder ROIs from the *ex vivo* FMI acquisition. All data are shown as mean ± SD, except the graphs showing the TRE in the brain *in vivo* at 30 min, 1 h and 3 h post-administration., the data showing the median (IQR). $^{**}P < 0.01$.

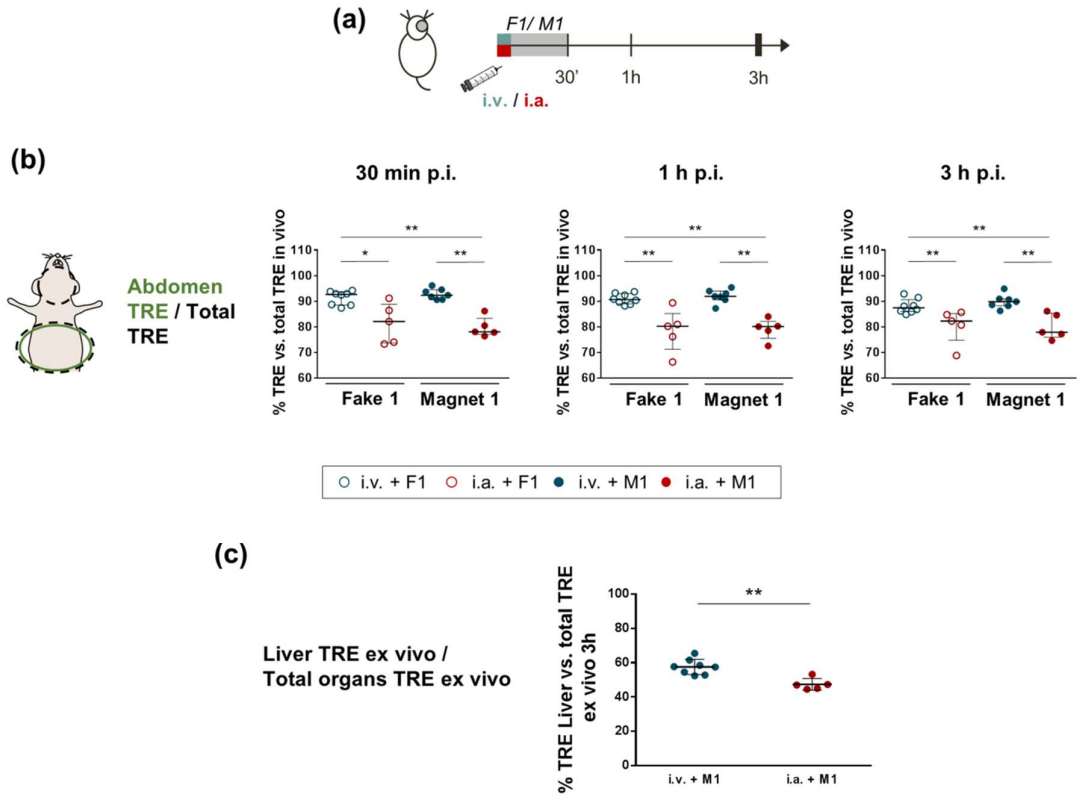

Figure S3. Non-target organs NC accumulation (complementary *Biodistribution study 1* data). (a) Scheme of the experimental design. (b) Graphs showing the quantification of the TRE percentage on the abdominal region ROIs versus the total TRE from all the ROIs drawn for each animal from *in vivo* FMI acquisitions at 30 min, 1 h and 3 h after NC administration. Data are shown as median (IQR). (c) Graph showing the quantification of the TRE percentage on the liver ROI versus the total TRE from all the organ ROIs drawn for each animal from the *ex vivo* FMI acquisition. Data are shown as mean ± SD. **P* < 0.05, ***P* < 0.01.

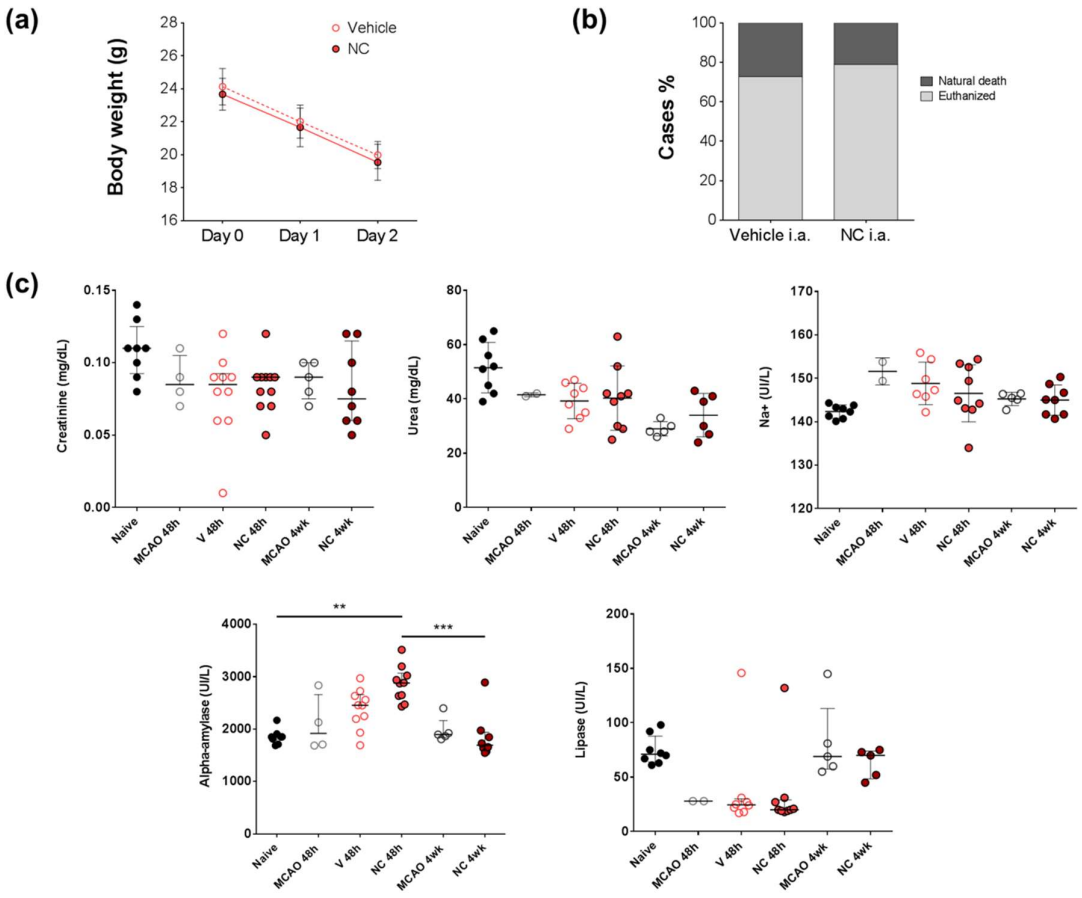

Figure S4. Complementary *Safety study* data. (a) Body weight follow-up during 48 h after vehicle or NC acute intraarterial-ICA administration in the MCAo model (*Safety study 1*). (b) Mortality rate after vehicle or NC intraarterial-ICA administration (*Safety study 1*). (c) Plasma levels of creatinine, urea, sodium, α-amylase and lipase at 48h and 4 weeks after MCAo and endovascular-ICA NC or vehicle administration (*Safety studies 1* and *2*). All data represented in graphs show the median (IQR), except the graphs representing the urea and sodium levels, showing the mean ± SD. ***P* < 0.01, ****P* < 0.001.

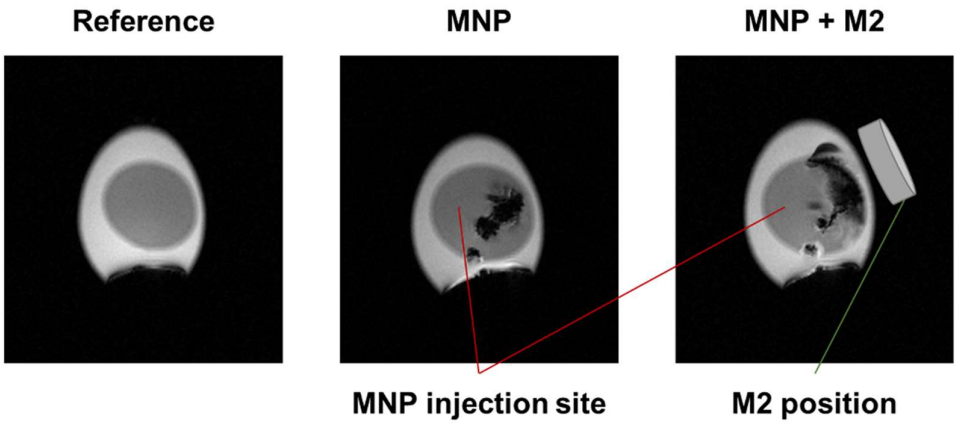

Figure S5. Magnetic targeting validation for M2. T2*WI for the magnetic fluid tracking of a magnetic fluid under the influence of the focused magnet M2 at 45 min after injection in a chicken egg model indicating the injection and magnet implantation sites.

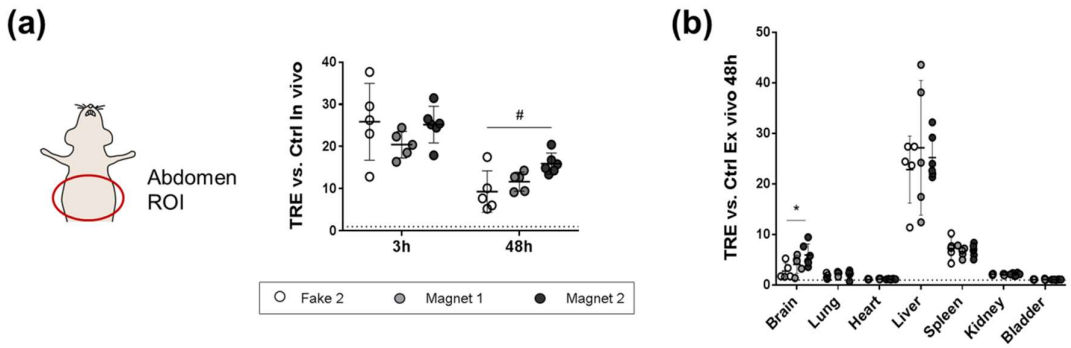

Figure S6. Complementary *Biodistribution study 3* data. (a) Graph showing the quantification of TRE on abdominal region ROIs corrected by their control animal from *in vivo* FMI acquisitions at 3 h and 48 h after intraarterial NC administration. (b) Graph showing the quantification of TRE on ROIs from organs imaged by FMI *ex vivo* after the last *in vivo* acquisition. Data are shown as mean ± SD. #$P < 0.1$, *$P < 0.05$.

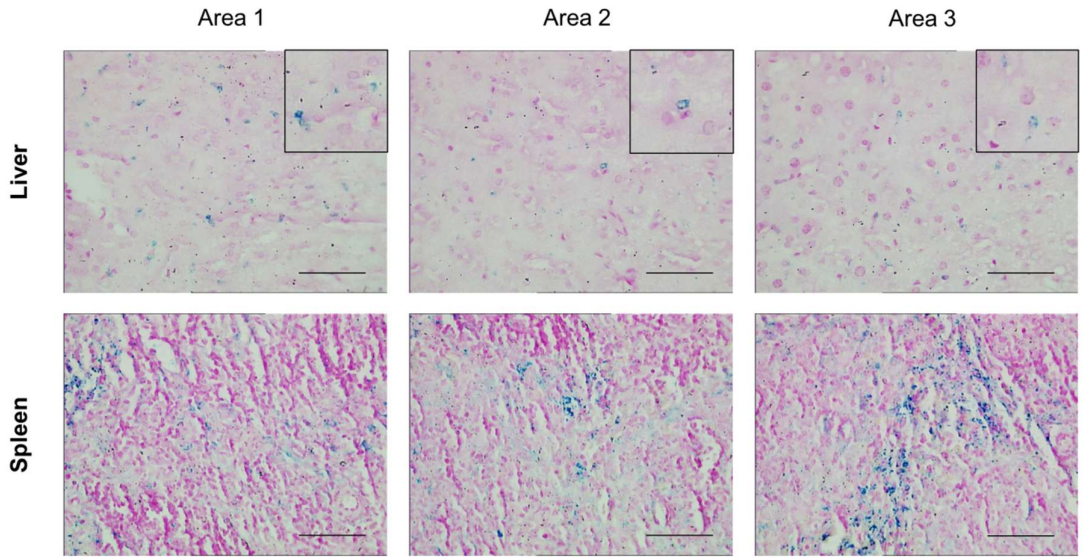

Figure S7. Verification of NC staining by Prussian blue. Liver and spleen slices were stained as controls of NC stain and endogenous ferric iron, respectively. Upper insets show magnified positive signals. Scale bar: 30 μm.